Anionic Species $(FH)_xF^-$ in Room-Temperature Molten Fluorides $(CH_3)_4NF\cdot mHF$

Yoshio Shodai,*,† Shinji Kohara,‡ Yasuo Ohishi,‡ Minoru Inaba,† and Akimasa Tasaka*,†

Department of Molecular Science and Technology, Faculty of Engineering, Doshisha University, 1−3 Miyakodani, Tadara, Kyotanabe, Kyoto 610-0321, Japan, and Japan Synchrotron Radiation Research Institute, 1-1-1 Kouto, Mikazuki-cho, Sayo-gun, Hyogo 679-5198, Japan

Received: September 2, 2003; In Final Form: December 17, 2003

Ionic and nonionic species in $(CH_3)_4NF\cdot mHF$ melts ($m = 3.0-5.0$) were investigated by ^1H NMR, IR spectroscopy, Raman spectroscopy, and high-energy X-ray diffraction measurements. Three types of anions, $(FH)F^-$, $(FH)_2F^-$, and $(FH)_3F^-$, were identified in these melts. The $(FH)_2F^-$ anion was thermodynamically the most stable of the complex anions in the $(CH_3)_4NF\cdot mHF$ ($3.0 \le m \le 5.0$), and its concentration was the highest. $(FH)_xF^-$ anions with $x = 4$ and 5 were not present at room temperature though the presence of $(FH)_xF^-$ ($x = 1-5$) has been known in the solid-state crystals. In the $(CH_3)_4NF\cdot mHF$ melts with $m = 3.0-5.0$, the number of HF combined with F^- is three or less, and excess HF exists as molecular HF.

Introduction

Molten fluoride systems such as $KF\cdot nHF$, $CsF\cdot nHF$, $NH_4F\cdot nHF$, etc. are important sources in chemical and electrochemical fluorination. These systems have been also excellent subjects to investigate strong hydrogen bonds. Thermochemical, spectroscopic, and diffraction studies of the solid-state alkali fluorides have revealed the presence of $(FH)F^-$ ($D_{\infty h}$ symmetry), $(FH)_2F^-$ (C_{2v} symmetry), and $(FH)_3F^-$ (D_{3h} symmetry) anions, which are formed by strong hydrogen bonding.[1−4] Mootz et al. determined the crystal structures of solid $(CH_3)_4NF\cdot mHF$ ($m =$ 2.0, 3.0, and 5.0) and found $(FH)_2F^-$, $(FH)_3F^-$, and $(FH)_5F^-$ anions by single-crystal X-ray diffraction measurements at low temperatures (−80 to −160 °C).[5] Shenderovich et al. confirmed the presence of $(FH)_2F^-$ and $(FH)_3F^-$ anions in solid $(nC_4H_9)_4NF\cdot mHF$ ($m = 2, 3$) dispersed in CDF_3/CDF_2Cl by NMR measurements at low temperatures (110−130 K).[6] Although it is expected that these anionic species exist in the molten fluorides containing excess HF at room temperature as well, no detailed study has been reported on the structure of anions in the room-temperature molten fluoride systems.

Recently, a new electrolyte system, $R_4NF\cdot mHF$ ($R = CH_3$, C_2H_5, nC_3H_7, and nC_4H_9, $m \ge 4$), has been used for partial fluorination of aromatic compounds such as benzene and xylene at room temperature.[7−10] The ionic conductivity of $(CH_3)_4NF\cdot mHF$ is constant in the m range of 2.0−3.0, whereas it increases linearly with an increase of m in the range of 3.0−5.5.[11] The $(CH_3)_4NF\cdot 4.0HF$ melt is the most suitable electrolyte for electrochemical fluorination because of its high ionic conductivity (197.6 mS cm^{-1} at 25 °C)[12] and a low HF vapor pressure. In a previous paper, we developed a new process for synthesis of gaseous $(CF_3)_3N$ using the $(CH_3)_4NF\cdot 4.0HF$ melt as an electrolyte.[13] The physicochemical properties of molten fluoride systems are strongly affected by the short-range and intermediate-range structures that maintain the microscopic interactions among ionic and/or nonionic species in the melt, and hence the structural analysis of the liquid is necessary to understand the electrochemical properties of the new room-temperature molten fluorides.

Many experimental techniques, such as infrared and Raman spectroscopy, NMR, etc., have been used to obtain detailed information on the structure of liquid. The structures of molten chloride systems, e.g., $NaCl-AlCl_3$, $KCl-AlCl_3$, and ethylmethylimidazolium chloride (EMICl)$-AlCl_3$, have been elucidated by spectroscopic measurements.[14−16] The structures of anhydrous HF and some molten fluoride systems have been investigated by the combination of the spectroscopic measurements and ab initio molecular dynamics simulation.[17−19]

Recently, high-energy X-ray diffraction using synchrotron radiation is an essential technique for structural study of disordered materials[20] and has already been applied to some liquids, water,[21,22] molten $ZnCl_2$,[23] and molten alkylimidazolium fluorohydrogenates.[24] These reports have proved that the high-energy X-ray diffraction technique enables us to obtain high-quality data in a wide scattering vector Q ($4\pi \sin\theta/\lambda$; 2θ, scattering angle; λ, wavelength of photons) range, which gives information on the short- and intermediate-range structures of species in the molten fluoride systems, with a high real-space resolution. Therefore, it is expected that combination of the spectroscopic measurements and the high-energy X-ray diffraction experiments allow us to determine the complicated structure of the molten fluorides.

In the present study, the structures of the room-temperature molten fluorides, $(CH_3)_4NF\cdot mHF$, were investigated by ^1H NMR measurements, IR spectroscopy, Raman spectroscopy, and high-energy X-ray diffraction experiments, in combination with ab initio molecular orbital calculation to identify ionic and nonionic species in the melts.

Experimental Section

$(CH_3)_4NF\cdot mHF$ melts ($m = 3.0$, 3.5, 4.0, 4.5, and 5.0) were prepared by feeding gaseous anhydrous HF (Morita Chemical Industries Co., Ltd.) through $(CH_3)_4NF\cdot 4.0HF$ (Morita Chemical Industries Co., Ltd.) or by mixing the $(CH_3)_4NF\cdot 4.0HF$ melt with $(CH_3)_4NF$ powder (Aldrich, purity > 97%). $NH_4F\cdot nHF$ melts ($n = 2.0$ and 3.0) were supplied by Morita Chemical

* To whom correspondence should be addressed. E-mail: atasaka@mail.doshisha.ac.jp (A.T.); eta1504@mail4.doshisha.ac.jp (Y.S.).

† Doshisha University.

‡ Japan Synchrotron Radiation Research Institute.

10.1021/jp036607u CCC: $27.50
Published on Web 01/21/2004

Industries Co., Ltd. ^{1}H NMR measurements were conducted with a JNM-GX400 spectrometer (400 MHz, JEOL) using acetonitrile-d_3 (0.75 ml, Euriso-top) as an external standard. The sample for NMR measurements was sealed in a PFA tube in order to obtain signals from a neat $(CH_3)_4NF\cdot m$HF melt, which was placed in an NMR sample tube (φ5 mm, Kusano Science Co.) filled with the deuteration solvent. IR spectra of the $(CH_3)_4NF\cdot m$HF melts were obtained with an IR-460 spectrometer (SHIMADZU). The sample was sandwiched between two AgCl crystals with a PTFE spacer (0.015 mm). Raman spectra of these melts were obtained with a T-64000 spectrometer (Jobin Yvon) using an Ar^+ ion laser (50 mW) as an excitation source. High-energy X-ray diffraction experiments were carried out using a wavelength of $\lambda = 0.2012$ Å ($E = 61.63$ keV) obtained from a Si 220 bent monochromator at SPring-8. The melts were encapsulated in a flat container of 3-mm thickness with polyethylene film windows. All the measurements were carried out at room temperature. The measured diffraction data were normalized to the Faber−Ziman total structure factors, $S(Q)$,[25] derived from the coherent scattering intensities, $I(Q)$, according to the following equation

$$I(Q) = \langle |f(Q)| \rangle^2 [S(Q) - 1] + \langle |f(Q)|^2 \rangle \quad (1)$$

where angular brackets represent the averages of overall atoms and $f(Q)$ is the X-ray form factor. The pair distribution functions, $g(r)$, were derived from the following function

$$g(r) = \frac{1}{2\pi^2 \rho r} \int_{Q_{min}}^{Q_{max}} Q[S(Q) - 1] \sin(Qr)\, dQ + 1 \quad (2)$$

where ρ is the total number density of the salts. The equilibrium geometries of $(FH)F^-$, $(FH)_2F^-$, and $(FH)_3F^-$ have already been reported by Kohara et al.[26] In the present study, ab initio MO calculations were carried out to derive the equilibrium geometries of NH_4^+, $(CH_3)_4N^+$, $(FH)_4F^-$, $(FH)_5F^-$, and HF. All MO calculations were performed using the Gaussian03W package.[27] The Hartree−Fock (HF) method with the 6-31G* basis set (HF/6-31G*)[28] was used in the geometry optimization of NH_4^+, $(CH_3)_4N^+$, $(FH)_4F^-$, $(FH)_5F^-$, and HF. The harmonic vibrational frequencies of all the species were calculated at the HF/6-31G* level. It is well known that vibrational frequencies calculated at HF/6-31G* are overestimated, and hence the values reported in the present study were scaled by 0.8929.[29] The intramolecular form factor, $F_1(Q)$, for $(CH_3)_4N^+$ was calculated from eq 3, in which the r values were estimated by ab initio MO calculation

$$F_1(Q) = \frac{1}{n\langle |f(Q)| \rangle^2} \sum_i \sum_j f_i(Q) f_j(Q) \exp(-b_{ij}Q^2) \frac{\sin(Qr_{ij})}{Qr_{ij}} + 1 \quad (3)$$

where r_{ij} is the atomic distance between i and j, b_{ij} is the pseudo-Debye−Waller factor for the mean thermal variation of r_{ij}, and n is the total number of atoms in a discrete ion.[24,30]

Result and Discussion

NMR Measurements. ^{1}H NMR spectra of the $(CH_3)_4NF\cdot m$HF melts ($m = 3.5$, 4.0, 4.5, and 5.0) measured at room temperature with acetonitrile-d_3 as an external standard are shown in Figure 1. The signal at 1.9 ppm is assigned to the residual protons of acetonitrile and the one at 2.6 ppm is assigned to the protons of the $(CH_3)_4N^+$ cation. The signal that appeared at around 10 ppm originates from the HF species. This signal shifted from 9.84 to 9.74 ppm with increasing the m value,

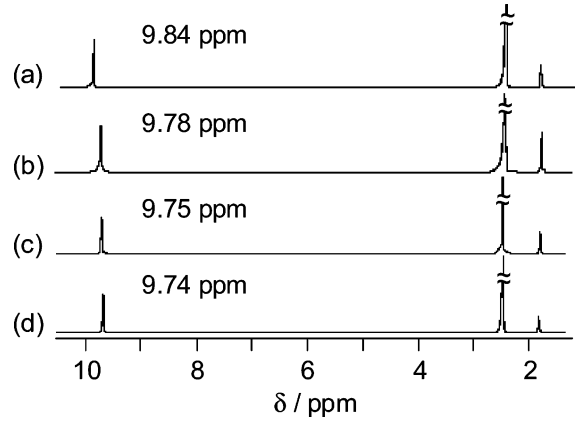

Figure 1. ^{1}H NMR spectra of $(CH_3)_4NF\cdot m$HF melt at room temperature. ($\delta_H = 1.93$), 400 MHz. (a) $(CH_3)_4NF\cdot 3.5$HF melt, (b) $(CH_3)_4NF\cdot 4.0$HF melt, (c) $(CH_3)_4NF\cdot 4.5$HF melt, and (d) $(CH_3)_4NF\cdot 5.0$HF melt.

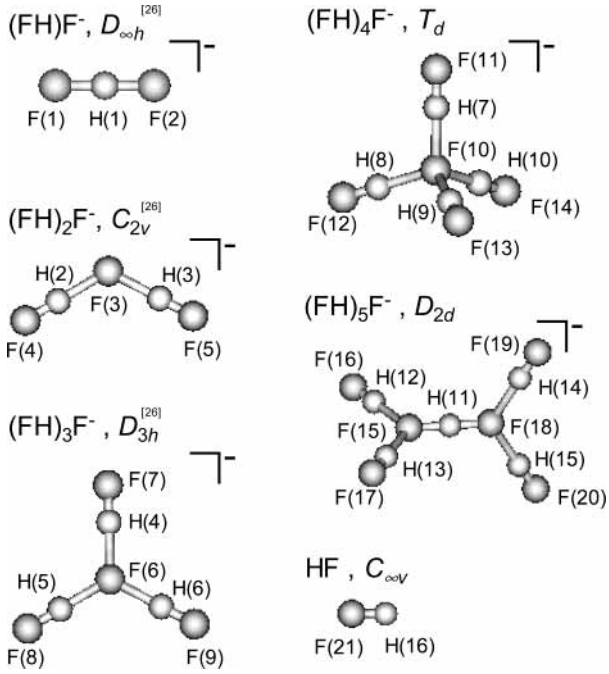

Figure 2. Structures of $(FH)_xF^-$ anions ($x = 1-5$) and HF molecule calculated by the ab initio calculations.

but the line width was unchanged even at low temperatures (0 to −80 °C). This shift implies a change in the concentration of the HF species in the melts. Although separate signals were confirmed for $(FH)_2F^-$ and $(FH)_3F^-$ in solid $(n\text{-}C_4H_9)_4NF\cdot m$HF at low temperatures (110−130 K) by Shenderovich et al.,[6] only a single sharp signal was observed for the HF species in each $(CH_3)_4NF\cdot m$HF melt. Since NMR does not have enough time scale (10^{-9} s) at room temperature to distinguish the $(FH)_xF^-$ ions in the melt, the results obtained above suggest rapid exchange of HF among molecular HF and $(FH)_xF^-$ anions in the melts, which are consistent with the results for the EMIF·2.3HF melt reported by Hagiwara et al.[31]

Ab Initio Calculations. Schematic illustrations for possible anionic species in the $(CH_3)_4NF\cdot m$HF melt, $(FH)F^-$, $(FH)_2F^-$, $(FH)_3F^-$, $(FH)_4F^-$, $(FH)_5F^-$, and molecular HF, calculated by ab initio MO calculations, are shown in Figure 2. The geometries of $(FH)_xF^-$ anions ($1 \le x \le 4$) are similar to those estimated from the ab initio molecular dynamics simulation reported by Rosenvinge et al.[32] The vibrational frequencies have no imaginary value for all anions. The calculated bond distances,

TABLE 1: Structure Parameters and Harmonic Vibrational Frequencies of $(FH)_xF^-$ Anions ($x = 1-5$)

$(FH)F^-$ $D_{\infty h}$	$(FH)_2F^-$ C_{2v}	$(FH)_3F^-$ D_{3h}	$(FH)_4F^-$ T_d	$(FH)_5F^-$ D_{2d}	
		Structural Parameters			
R[H(1)−F(1)] = 1.125 Å	R[H(2)−F(4)] = 0.981 Å	R[H(4)−F(7)] = 0.953 Å	R[H(7)−F(1))] = 0.998 Å	R[H(11)−F(15)] = 1.121 Å	
R[F(1)−F(2)] = 2.253 Å	R[F(3)−F(4)] = 2.349 Å	R[H(4)−F(6)] = 1.472 Å	R[H(7)−F(10)] = 1.553 Å	R[F(15)−F(18)] = 2.242 Å	
	R[H(2)−F(3)] = 1.369 Å	R[F(6)−F(7)] = 2.425 Å	R[F(10)−F(11)] = 2.491 Å	R[H(12)−F(15)] = 1.611 Å	
				R[H(12)−F(16)] = 0.931 Å	
				R[F(15)−F(16)] = 2.542 Å	
	∠H(2)F(3)H(3) = 117.5°	∠H(4)F(6)H(5) = 120.0°	∠H(7)F(10)H(8) = 109.5°	∠H(11)F(15)H(12) = 119.4°	
				∠H(12)F(15)H(17) = 121.2°	
		Harmonic Vibrational Frequencies (cm^{-1})			
597(σ_g)	45 (A_1)	15 (A_2'')	29 (E)	11 (B_1)	702 (E)
	347 (A_1)	37 (E)	41 (T_2)	21 (E)	747 (B_2)
	372 (B_2)	38 (E)	223 (A_1)	31 (A_1)	783 (A_1)
	981 (B_2)	245 (A_1')	285 (T_2)	44 (B_2)	1185 (E)
	989 (A_2)	333 (E′)	692 (T_1)	51 (E)	1262 (B_2)
	1030 (B_1)	815 (A_2')	843 (E)	197 (B_2)	3482 (E)
	1109 (A_1)	849 (E″)	863 (T_2)	207 (A_1)	3553 (B_2)
	2466 (B_2)	907 (A_2'')	3329 (T_2)	272 (E)	3572 (A_1)
	2758 (A_1)	959 (E)	3519 (A_1)	606 (A_1)	
		3026 (E′)		657 (A_2)	
		3250 (A_1')		667 (B_1)	

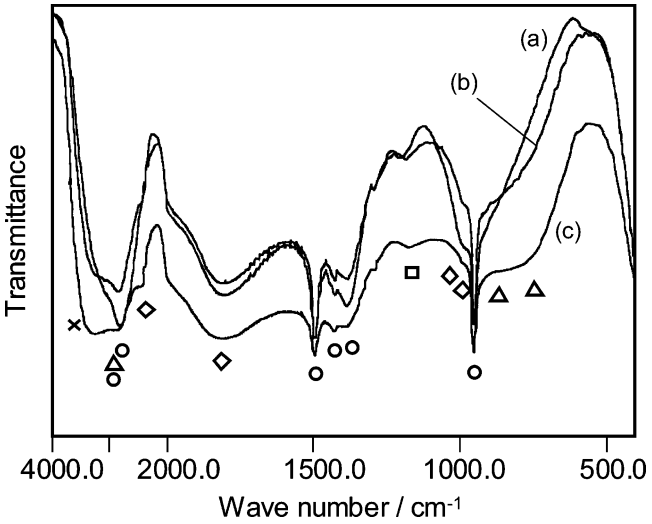

Figure 3. IR spectra of $(CH_3)_4NF\cdot m$HF melts at room temperature. (a) $(CH_3)_4NF\cdot 3.5$HF melt, (b) $(CH_3)_4NF\cdot 4.0$HF melt, and (c) $(CH_3)_4NF\cdot 4.5$HF melt. Peak positions of $(CH_3)_4N^+$ (○), $(FH)F^-$ (□), $(FH)_2F^-$ (◇), $(FH)_3F^-$ (△), and molecular HF (×) are shown in the figure.

TABLE 2: Frequencies of IR-Active Absorption Maxima in the IR Spectra of the $(CH_3)_4NF\cdot m$HF Melt

species	obsd (cm^{-1}) this work	obsd (cm^{-1}) previous work		calcd[a] (cm^{-1})	
$(CH_3)_4N^+$ (T_d)	940, vs	970,[33] vs	1027[38]	919	(T_2)
	1300, w	1209,[33] w	1288[38]	1281	(T_2)
	1375, vw	1312,[33] vvw	1436[38]		(T_2)
	1420, m	1415,[33] m	1578[38]	1418	(T_2)
	1480, vs	1490,[33] sh	1647[38]	1481	(T_2)
	2810, s, br	2822,[33] s, br		2902	(T_2)
	3000, br	3030,[33] s, br		2996	(T_2)
$(FH)F^-$ ($D_{\infty h}$)	1190, vw	1223[34]		1218	(σ_g)
		1450[34]		1222	(σ_u)
$(FH)F^-$ (C_{2v})	∼500, m	455[35]		372	(B_2)
	1000, w	1020[35]		981	(B_2)
	1050, w	1050[35]		1030	(B_2)
	1800, s, br	1770[35]		2758	(A_1)
	2500, m	2000[35]		2466	(B_2)
$(FH)_3F^-$ (D_{3h})	875, m, br			910	(A_2'')
	2900, m, br			962	(E')
				3036	(E')
HF ($C_{\infty v}$)	3450, s, br	3961[39] [b]	3590[39] [c]	3878	(d)

[a] Calculated at the Gaussian03W HF/6-31G* level. [b] Gaseous HF. [c] Liquid HF.

bond angles, and harmonic vibrational frequencies for the $(FH)_xF^-$ anions are summarized in Table 1. The distances between the central and terminal fluorine atoms in $(FH)_xF^-$ anions, e.g., R[F(1)−F(2)], R[F(3)−F(4)], R[F(6)−F(7)], R[F(10)−F(11)], and R[F(15)−F(16)] in Figure 2, were 2.253, 2.349, 2.425, 2.491, and 2.542 Å, respectively, and became longer with increasing of x in $(FH)_xF^-$.

IR and Raman Spectroscopy. The IR spectra of $(CH_3)_4NF\cdot m$HF melts ($m = 3.5$, 4.0, and 4.5) are shown in Figure 3. The position for each absorption band was almost unchanged in the range of $3.5 \le m \le 4.5$. The frequencies of the observed absorptions are summarized with the results of the ab initio calculation in Table 2. It is well known that $(CH_3)_4N^+$ has T_d symmetry and 19 fundamental vibrations of $3A_1 + A_2 + 4E + 4T_1 + 7T_2$, and only the seven T_2 modes are IR active. The absorption bands of the $(CH_3)_4N^+$ cation were observed at around 940, 1300, 1375, 1420, 1480, 2810, and 3000 cm^{-1} in each melt, which are consistent with those reported for crystalline $(CH_3)_4NF$.[33] The others were broad absorption bands or shoulders and are assigned to $(FH)_xF^-$ and molecular HF. These absorptions were observed at 1190 cm^{-1} for $(FH)F^-$ anion at 500, 1000, 1050, 1800, and 2500 cm^{-1} for the $(FH)_2F^-$ anion and at 875 and 2900 cm^{-1} for the $(FH)_3F^-$ anion, which is in good agreement with the results of the ab initio calculation and/or the experimental data reported in the literature.[34,35] The ν-(A_1) band of $(FH)_2F^-$ observed at 1800 cm^{-1} was shifted downward by about 1000 cm^{-1} from the calculated value (2758 cm^{-1}). The reason for this large difference is not clear. The shoulder peak between 3600 and 3800 cm^{-1} indicated the presence of molecular HF in the melts. Furthermore, its

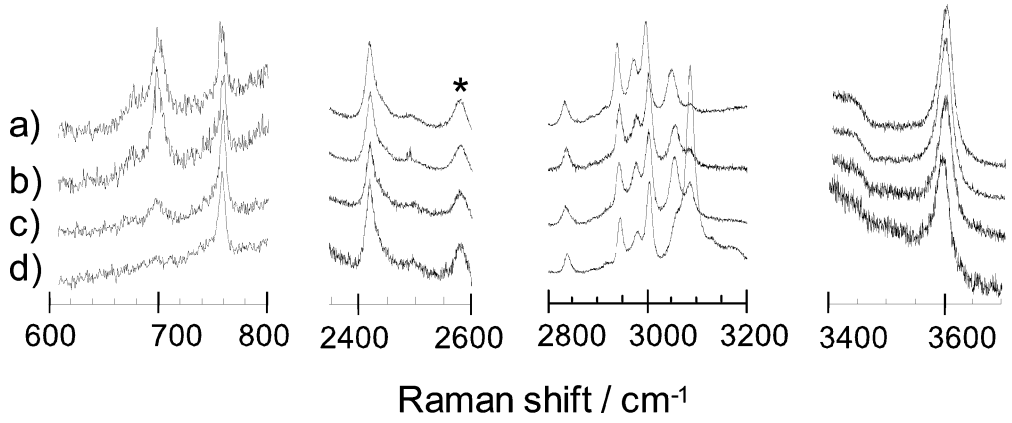

Figure 4. Raman spectra of $(CH_3)_4NF{\cdot}m$HF melts at room temperature. (a) $m = 3.5$, (b) $m = 4.0$, (c) $m = 4.5$, and (d) $m = 5.0$. The asterisk indicates a silica glass cell.

absorbance increased with increasing the m value in $(CH_3)_4NF{\cdot}m$HF, which suggests that the amount of molecular HF increased with an increase in m. Though only a single peak was observed for these HF species in NMR spectra as mentioned earlier, many absorptions of ionic and nonionic species could be distinguished in all melts because the time scale of IR (10^{-13} s) is much faster than the exchange rate of HF among molecular HF and $(FH)_xF^-$ anions.

Raman spectra of the $(CH_3)_4NF{\cdot}m$HF melts are shown in Figure 4, in which the spectra are divided into four regions for clarity. These results also revealed the presence of $(FH)F^-$, $(FH)_2F^-$, and $(FH)_3F^-$ anions and molecular HF. The Raman peaks of the $(CH_3)_4N^+$ cation at 760, 2835, 2940, 2980, and 3050 cm^{-1} agree well with those of solid $(CH_3)_4NF$ reported by Christe et al.[33] The peak at 700 cm^{-1} is assigned to the $\nu(\Sigma_g)$ band of the $(FH)F^-$ anion. The intensity of this peak decreased with an increase in the m value, and the peak disappeared in the $(CH_3)_4NF{\cdot}5.0$HF melt. Likewise, the presence of $(FH)_2F^-$ anion is confirmed from the $\nu(B_2)$ band at 2420 cm^{-1} in all melts. The peak intensity of this band was almost unchanged when the m value was changed, which demonstrates that the $(FH)_2F^-$ anion exists stably in the $(CH_3)_4NF{\cdot}m$HF melts ($m = 3.5-5.0$). The peak at around 3080 cm^{-1} is assigned to the $\nu(E')$ band of the $(FH)_3F^-$ anion, and its peak intensity increased with increasing the m value; particularly, the peak in the $(CH_3)_4NF_5.0$HF melt was remarkable. This decreasing tendency of $(FH)_3F^-$ is in contrast with the decreasing tendency of FHF^- with increasing m. On the other hand, $(FH)_4F^-$ and $(FH)_5F^-$ anions, the presence of which have been reported in the solid $KF{\cdot}4.0$HF and $(CH_3)_4NF{\cdot}5.0$HF,[5,36] were not detected in these melts by IR and Raman spectroscopy. These results indicate that the number of HF combined with F^- is three or less, and excess HF exists as molecular HF in the $(CH_3)_4NF{\cdot}m$HF melts. The peak of the molecular HF could be observed at around 3600 cm^{-1},[1] whereas the harmonic frequency for molecular HF obtained by the ab initio calculation was 3878 cm^{-1}. In general, the frequency shift on the IR spectrum can be explained in terms of altered bond strength or atomic masses. It is widely known that HF is polymerized in neat HF liquid because of hydrogen bonding among HF molecules. In the case of molecular HF in the $(CH_3)_4NF{\cdot}m$HF melts, the bond strength between H and F atoms must be affected by additional hydrogen bonding with $(FH)_xF^-$ anions that exist in the neighborhood. The presence of hydrogen bonding in the melts is the reason for the observed frequency shift of the HF peak.

High-Energy X-ray Diffraction. The total structure factors, $S(Q)$, of the $NH_4F{\cdot}n$HF ($n = 2.0$ and 3.0) and $(CH_3)_4NF{\cdot}m$HF ($m = 3.0$, 4.0, and 5.0) melts are shown in Figure 5, together

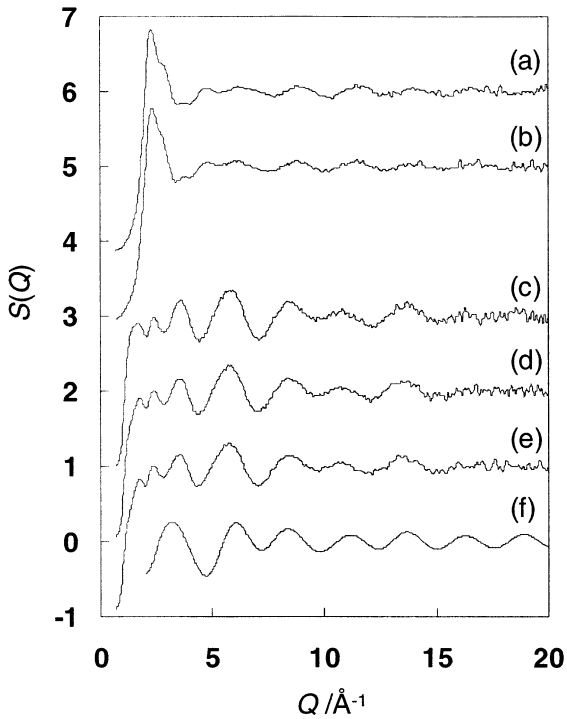

Figure 5. Total structure factors, $S(Q)$, of $NH_4F{\cdot}n$HF and $(CH_3)_4NF{\cdot}m$HF melts and calculated intramolecular form factor, $F_1(Q)$, of $(CH_3)_4N^+$. Successive curves are displaced upward for clarity. (a) $NH_4F{\cdot}2.0$HF melt, (b) $NH_4F{\cdot}3.0$HF melt, (c) $(CH_3)_4NF{\cdot}3.0$HF melt, (d) $(CH_3)_4NF{\cdot}4.0$HF melt, (e) $(CH_3)_4NF{\cdot}5.0$HF melt, and (f) $(CH_3)_4N^+$.

with the intramolecular form factor, $F_1(Q)$, of $(CH_3)_4N^+$ calculated using eq 3. The first sharp diffraction peak (FSDP) associated with a shoulder was observed at around $Q = 2.3$ $Å^{-1}$ in both $NH_4F{\cdot}n$HF melts. They were very similar, though HF molar concentrations were different. Since the weighting factors of N−H and H−H correlations for X-rays are very small, it is considered that the weak oscillations at $Q \geq 4$ $Å^{-1}$ were mainly contributed by intramolecular correlation of the F−F correlation in $(FH)_xF^-$ anions. However, the oscillations of the total structure factors were weaker than expected, which suggests that the F−F correlations in $(FH)_xF^-$ anions are highly disordered. On the other hand, the $S(Q)$ of the $(CH_3)_4NF{\cdot}m$HF melts showed more significant oscillations than those of the $NH_4F{\cdot}n$HF melts. Three peaks observed at $Q \leq 5$ $Å^{-1}$ imply the intermolecular correlations of the $(CH_3)_4N^+$ cation in the melts. The oscillations at $Q \geq 5$ $Å^{-1}$ in the $(CH_3)_4NF{\cdot}m$HF melts are mainly due to the tetrahedral NC_4 short-range structure because the calculated intramolecular form factor, $F_1(Q)$, of

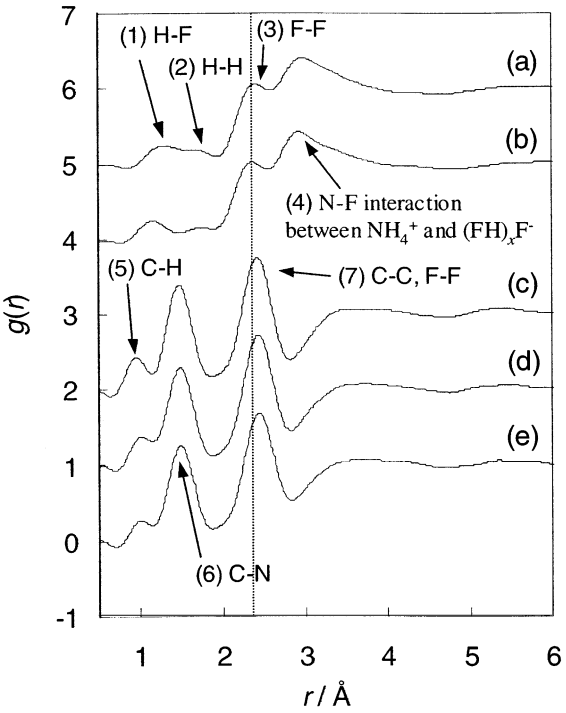

Figure 6. Pair distribution functions, $g(r)$, of $NH_4F{\cdot}n$HF and $(CH_3)_4NF{\cdot}m$HF melts. All data are displaced upward for clarity. (a) $NH_4F{\cdot}$2.0HF melt, (b) $NH_4F{\cdot}$3.0HF melt, (c) $(CH_3)_4NF{\cdot}$3.0HF melt, (d) $(CH_3)_4NF{\cdot}$4.0HF melt, and (e) $(CH_3)_4NF{\cdot}$5.0HF melt.

$(CH_3)_4N^+$ agrees well with experimental total structure factors at $Q \geq 5$ Å^{-1}. It is suggested from these results that F−F correlations in these melts were also disordered.

Figure 6 shows the pair distribution functions, $g(r)$, of the $NH_4F{\cdot}n$HF and $(CH_3)_4NF{\cdot}m$HF melts. Two peaks observed at 1.1 and 1.7 Å (peaks 1 and 2) indicate the N−H and H−H correlations, respectively, of the NH_4^+ cation, probably overlapped with H−F correlations that consist of $(FH)_xF^-$ anions. However, these weak peaks are strongly affected by ripples from truncation errors of Fourier transformation, so that it is difficult to give more detailed analysis. The peak at 2.36 Å (peak 3) is assigned to F−F correlations of the $(FH)_xF^-$ anion in the $NH_4F{\cdot}$2.0HF melt because only the F−F correlations in the $(FH)_xF^-$ anions have a peak at around 2.36 Å. Moreover, the position of this peak suggests that the $(FH)_2F^-$ anion may be the major anionic species in the $NH_4F{\cdot}$2.0HF melt, considering that the distance of F−F correlations for $(FH)_xF^-$ anions ($x = 1-5$) are 2.253, 2.349, 2.425, 2.491, and 2.542 Å, respectively. The peak at 3.0 Å (peak 4) indicates the distance of the N−F interaction between NH_4^+ and $(FH)_xF^-$ ions in the liquid state because its distance in the NH_4F crystal is 2.8 Å.[37] In the $g(r)$ for the $NH_4F{\cdot}$3.0HF melt, the peak assigned to the F−F correlation in the $(FH)_xF^-$ anion shifted to 2.40 Å from 2.36 Å in that for a $NH_4F{\cdot}$2.0HF melt. This feature indicates that not only the $(FH)_2F^-$ anion but also the $(FH)_3F^-$ anion exists in the $NH_4F{\cdot}$3.0HF melt. On the other hand, the presence of the $(FH)F^-$ anion, which has the shortest F−F correlation in $(FH)_xF^-$, could not be confirmed clearly because the peak and/or shoulder did not appear at around 2.3 Å in the $g(r)$ of the $NH_4F{\cdot}n$HF melt. Assuming that its correlation was overlapped with the peak 3, the amount of $(FH)F^-$ anion may be small since it exists in the $NH_4F{\cdot}n$HF melts.

The peaks at 1.1 and 1.5 Å (peaks 5 and 6) in $g(r)$ of the $(CH_3)_4NF{\cdot}m$HF melts are assigned to the C−H and C−N correlations, respectively. On the other hand, the results of the ab initio calculation revealed that the peak at around 2.4 Å (peak 7) consisted of the C−C correlation in the cation and the F−F correlation in the $(FH)_2F^-$ and/or $(FH)_3F^-$ anions. The peak appeared at 2.42 Å in the $g(r)$ of the $(CH_3)_4NF{\cdot}$3.0HF melt and shifted to 2.43 and 2.44 Å in $(CH_3)_4NF{\cdot}$4.0HF and $(CH_3)_4NF{\cdot}$5.0HF, respectively. This fact is in good agreement with the results obtained by IR and Raman measurements; that is, while the $(FH)_3F^-$ anion is thermodynamically the most stable and its concentration was the highest, the amount of $(FH)_3F^-$ increases with increasing the m value in $(CH_3)_4NF{\cdot}m$HF.

Conclusion

The structures of $(CH_3)_4NF{\cdot}m$HF melts were investigated by NMR, IR spectroscopy, Raman spectroscopy, and high-energy X-ray diffraction measurements to determine the ionic and nonionic species in these melts. In these melts, three types of anions, $(FH)F^-$, $(FH)_2F^-$, and $(FH)_3F^-$, were identified. Of these, $(FH)_2F^-$ anion was thermodynamically the most stable, and its concentration was the highest in the liquid state of the $(CH_3)_4NF{\cdot}m$HF. $(FH)_4F^-$ and $(FH)_5F^-$ anions, the presence of which has been confirmed in the solid $(CH_3)_4NF{\cdot}m$HF, were not detected in these melts, though $(CH_3)_4NF{\cdot}m$HF ($m = 4.0$ or 5.0) contains excess HF. The excess HF exists as a molecular HF molecule in these melts. The exchange of HF molecule among nearby molecular HF and $(FH)_xF^-$ anions occurs in the melts and its rate is faster than the time scale of NMR measurements (10^{-9} s) and slower than that of IR and Raman measurements (10^{-13} s).

Acknowledgment. The authors thank Dr. Momota at Morita Chemical Industries, Co., Ltd., for his help and advice on NMR measurements. They also wish to express many thanks to Dr. T. Abe at Kyoto University for his supports on Raman measurements and ab initio calculations. The synchrotron radiation experiments were performed at the SPring-8 with the approval of the Japan Synchrotron Radiation Research Institute (Proposal No. 2002B0070-ND1-np). This work was supported by scholarship contribution of Mitsui Chemicals, Inc., Grant-in-Aid for Scientific Research (C) (No. 15550131) from Japan Society for the Promotion of Science, and Aid of Doshisha University's Research Promotion Fund in 2001.

References and Notes

(1) Cady, G. H. *J. Am. Chem. Soc.* **1943**, *56*, 1431.
(2) Hamrmon, K. M.; Gennick, I. *J. Mol. Struct.* **1977**, *38*, 97.
(3) Morrison, J. S.; Jache, A. W. *J. Am. Chem. Soc.* **1959**, *81*, 1821.
(4) Adamczak, R. L.; Mattern, J. L.; Tieckelmann, H. *J. Phys. Chem.* **1959** *63*, 2063.
(5) Mootz, D.; Boenigk, D. *Z. Anorg. Allg. Chem.* **1987**, *544*, 159.
(6) Shenderovich, I. G.; Limbach, H.; Smirnov, S. N.; Tolstoy, P. M.; Denisov, G. S.; Golubev, N. S. *Phys. Chem. Chem. Phys.* **2002**, *4*, 5488.
(7) Momota, K.; Morita, M.; Matsuda, Y. *Electrochim. Acta* **1993**, *38*, 1123.
(8) Momota, K.; Kato, K.; Morita, M.; Matsuda, Y. *Electrochim. Acta* **1994**, *39*, 681.
(9) Momota, K.; Yonezawa, T.; Hayakawa, Y.; Kato, K.; Morita, M.; Matsuda, Y. *J. Appl. Electrochem.* **1995**, *25*, 651.
(10) Momota, K.; Mukai, K.; Kato, K.; Morita, M. *Electrochim. Acta* **1998**, *43*, 2503.
(11) Tasaka, A.; Shodai, Y.; Yamashita, J.; Kinumoto, T.; Miyasaka, A.; Momota, K.; Ibuki, K.; Ueno, M. Proceedings of 6th International Symposium on Molten Salt Chemistry and Technology, 2001, p 328.
(12) Momota, K.; *Molten Salts* **2002**, *45*, 42.
(13) Tasaka, A.; Yachi, T.; Makino, T.; Hamano, K.; Kimura, T.; Momota, K. *J. Fluorine Chem.* **1999**, *97*, 253.
(14) Syvin, S. J.; Klaeboe, P.; Rytter, E.; Øye, H. A. *J. Chem. Phys.* **1970**, *52*, 2776.
(15) Tait, S.; Osteryoung, R. A. *Inorg. Chem.* **1984**, *23*, 4352.
(16) Takahashi, S.; Curtiss, L. A.; Gosztola, D.; Koura, N.; Saboungi, M.-L. *Inorg. Chem.* **1995**, *34*, 2990.

(17) Röthlisberger, U.; Parrinello, M. *J. Chem. Phys.* **1997**, *106*, 4658.
(18) Kreitmeir, M.; Bertagnolli, H.; Mortensen, J. J.; Parrinello, M. *J. Chem. Phys.* **2003**, *118*, 3639.
(19) Simon, C.; Cartailler, T. Turq, P. *Phys. Chem. Chem. Phys.* **2001**, *3*, 3119.
(20) Ohno, H.; Kohara, S.; Umesaki, N.; Suzuya, K. *J. Non-Cryst. Solid* **2001**, *293*−*295*, 125.
(21) Badyal, Y. S.; Saboungi, M.; Price, D. L.; Shastri, S. D.; Haeffner, D. R.; Soper, A. K. *J. Chem. Phys.* **2000**, *112*, 9206.
(22) Lie, G. C.; Clementi, E. *J. Chem. Phys.* **1976**, *64*, 5308.
(23) Neuefeind, J.; Todheide, K.; Lemke, A.; Bertagnolli, H. *J. Non-Cryst. Solid* **1998**, *224*, 205.
(24) Hagiwara, R.; Matsumoto, K.; Tsuda, T.; Ito, Y.; Kohara, S.; Suzuya, K.; Matsumoto, H.; Miyazaki, Y. *J. Non-Cryst. Solids* **2002**, *312*−*314*, 414.
(25) Faber, T. E.; Ziman, J. M. *Philos. Mag.* **1965**, *11*, 153.
(26) Kohara, S.; Hagiwara, R.; Matsumoto, K.; Ito, Y.; Kajinami, A.; Suzuya, K. *Molten Salt XIII* **2002**, 1047.
(27) Frisch, M. J., et al. Gaussian03; Gaussian Inc.: Pittsburgh, PA, 2003.
(28) Beinning, R. C., Jr.; Curtiss, L. A. *J. Comput. Chem.* **1990**, *11*, 1206.
(29) Pople, J. A.; Krishnan, R. *Int. J. Quantam Chem., Symp.* **1981**, *15*, 269.
(30) Takahashi, S.; Suzuya, K.; Kohara, S.; Koura, N.; Curtiss, L. A.; Sabounji, M. L. *Z. Phys. Chem.* **1999**, *209*, 209.
(31) Hagiwara, R.; Hirashige, T.; Tsuda, T.; Ito, Y. *J. Electrochem. Soc.* **2002**, *149*, D1−D4.
(32) von Rosenvinge, T.; Parrinello, M.; Klein, M. L. *J. Chem. Phys.* **1997**, *107*, 8012.
(33) Christe, K. O.; Wilson, W. W.; Wilson, R. D.; Bau, R.; Feng, J. *J. Am. Chem. Soc.* **1990**, *112*, 7619.
(34) Coté, G. L.; Thompson, H. W. *Proc. R. Soc. London* **1952**, *210A*, 206.
(35) Ažman, A.; Ocvirk, A.; Hadži, D.; Giguère, P. A.; Schneider, M. *Can. J. Chem.* **1967**, *45*, 1347.
(36) Coyle, B. A.; Schroeder, L. W.; Ibers, J. A. *J. Solid State Chem.* **1970**, *1*, 386.
(37) Reeuwijk, S. J.; Beek, K. G.; Feil, D. *J. Phys. Chem. A* **2000**, *104*, 10901.
(38) Boldyrev, A. I.; Simons, J. *J. Chem. Phys.* **1992**, *97* (9), 6621.
(39) Siebert, H. *Anwendungen der Schwingungsspektroskopie in der Anorganischen Chemie*; Springer-Verlag: Berlin, 1966; pp 38−52.